Dominant updriftward sediment transport on the updrift-side of a modern deflected delta, Ishikari coast, Hokkaido, Japan

Emmanuel Poizot, Gentaro Kawakami, Kenji Nishina

(ARTICLE)

Dominant updriftward sediment transport on the updrift-side of a modern deflected delta, Ishikari coast, Hokkaido, Japan

Gentaro Kawakami[a, *], Kenji Nishina[a] and Emmanuel Poizot[b]

[a]*Geological Survey of Hokkaido, Kita 19 Nishi 12, Kita-ku, Sapporo 060-0819, Japan*

[b]*Cnam/Intechmer-LUSAC, Digue de Collignon, 50110 Tourlaville, Cherbourg-en-Cotentin, France*

*Corresponding Author
E-mail address: kawakami-gentaro@hro.or.jp (G. Kawakami)

ABSTRACT

The Ishikari coast of Hokkaido, Japan is a wave-dominated semi-enclosed coast, the sediments of which are primarily sourced from a single river (the Ishikari River), forming a northeast deflected delta. Asymmetric and deflected deltas are generally considered to be formed under net longshore sediment transport *downdriftward*; however, through sedimentological and grain-size trend analysis (GSTA) of seafloor sediments, along with some other observational data, we recognized dominant *updriftward* sediment transport on the updrift-side of the deflected delta system. GSTA showed that the most important trend in the coast is coarser, better-sorted, and more positively skewed (CB+). CB+ trends around the river mouth converge from the lower shoreface zone to the river mouth spit on the updrift side. The trends reflect the combined effects of shore-normal wave action and river sediment discharge. Wave-driven surface currents crossing over the delta lobe converge at the southwestern side of the river mouth. In the deeper zone (lower shoreface), southwest (updriftward) oriented CB+ trends prevail. These trends reflect successive re-deposition of delta front sands, with progressive mud winnowing, driven by the strong south-westerly bottom currents observed in the bay during winter storms. Although GSTA did not show any apparent trend field in the nearshore zone, gradual fining of sand fractions to the southwest, along with the chronological transition of the coastline after the construction of a large port, suggest a dominant longshore sediment transport updriftward on the updrift-side of the delta. Because the growth of deflected deltas depends on dominant sediment accretion on the updrift-side, these results can be rationalised in the case of internally sourced deflected deltas. Uncertainties remain regarding the net alongshore sediment transport of the entire Ishikari coast; however, the deflected planform is controlled by deflected mouth bars and river mouth jets due to the waves approaching the river mouth at slightly oblique angle in winter, and is likely independent on the direction of dominant sediment transport.

Keywords deflected delta, grain-size trend analysis, Ishikari Coast, sediment pathway, wave-influenced delta

1. Introduction

Coastal regions are often the site of large cities and concentrated human activities, especially delta plains have been highly developed for land use. However, recent global environmental changes due to human impact are significantly affecting delta morphology (Anthony, 2015; Nienhuis et al., 2020). Therefore, it is important to gain a detailed understanding of sedimentary processes of delta systems to support predictive environmental planning, sustainable development, and hazard mitigation (e.g., Kairytė and Stevens, 2015; Nienhuis et al., 2020).

Recent advances in our understanding of wave-influenced delta systems have helped improve their classification based on their planforms and facies architectures: symmetric, asymmetric, or deflected (Bhattacharya and Giosan, 2003; Bhattacharya, 2006; 2010). Asymmetric and deflected deltas are thought to grow via sustained downdriftward longshore currents generated by an oblique wave approach to the coastline (Dominguez, 1996; Reading and Collinson, 1996; Bhattacharya and Giosan, 2003; Bhattacharya, 2006; 2010). In case of these deltas, predominant sediment accretions on the updrift side are needed, and it is generally explained by a trapping of externally sourced sediments in the updrift side by the groin effect of river mouth (Reading and Collinson, 1996; Rodriguez et al., 2000; Bhattacharya and Giosan, 2003). However, the asymmetric and deflected delta models are still conceptual, and the hydrodynamic processes and resulting sediment distributions of real systems exhibit much more complex variations (see Anthony, 2015 and references therein). For example, the modern asymmetric Mitchell River Delta, Gulf of Carpentaria, Australia, has a northward-deflected planform, whereas the mouth bar sediments show southward-dipping cross-stratification opposite the expected direction (Ainsworth et al., 2016). Difficulties in determining the sources, pathways, and final emplacement of sediments in deflected deltas have hindered our understanding of the detailed growth mechanisms of such systems (Anthony, 2015; Korus et al., 2015). In addition, it should be noted that

the definition of the updrift and downdrift sides of deflected deltas often depends only on geomorphic features, not the actual direction of net sediment transport. In this study, the adjective terms "updrift" and "downdrift" are also used in this way (i.e., geomorphic direction).

The coast along the eastern margin of the Japan Sea is characterised by a low tidal range and high wave energy and hosts several strand plains and delta systems. Among these, the Ishikari coast of Hokkaido, northern Japan, consists of a highly deflected delta at the mouth of the Ishikari River (Fig. 1). The delta has been developing under the late Holocene high-stand condition after the Mid-Holocene sea-level maximum (Ohshima et al., 1978; Matsushita, 1979). The coast is situated within a bay bordered by rocky projecting land masses, and most of the sediment inputs originate solely from the Ishikari River (e.g., Ohshima and Yokota, 1978). This single source condition enables to interpret sediment pathways more certainly as no other inputs can scramble the dominated transport signal.

The Ishikari Bay bottom sediments are mainly under the action of wind-driven currents during winter storms; hence, its analysis should highlight the seasonal storm impact on the granulometric sorting. In the present work, we conducted a grain size trend analysis (GSTA) following the method of Poizot and Méar (2010), which has been shown to successfully visualise sediment pathways (Maillet et al., 2011; Kairytė and Stevens, 2015). Though STA® (McLaren, 1981) and GSTA approaches have had successive modifications on some of their aspects, only a small number of studies have scrutinised the validity of McLaren's initial theory and trend cases definitions. Gao et al. (1994), Asselman (1999), Carriquiry and Sanchez (1999), Carriquiry et al. (2001), Rios et al. (2002), Poizot et al. (2013) found different trend cases than the initial McLaren's ones under particular conditions. Poizot and Méar (2010) provided a software tool to perform a GSTA approach in which no prior choice of trend case was made, thus enabling an exploratory approach in choosing a single or combined trend case.

102 The backgrounds of studied area are introduced in Section 2. The Section 3 gives
103 details of the laboratory analysis, numerical treatments of the data set, and GSTA.
104 Finally, results (Section 4) and discussions (Section 5) explain our understanding of the
105 sediment transport processes in the Ishikari bay, before the conclusion in Section 6.
106

107 ## 2. Regional Setting

108 The Ishikari delta, Hokkaido, northern Japan, is located in the inner area of Ishikari
109 Bay (Fig. 1). The 30 km-long sandy coastline, oriented northeast–southwest, curves
110 gently landward, and slightly protuberates seaward at the mouth of the Ishikari River as
111 a northeast deflected planform. Rocky projecting land masses border the coast on both
112 the southwestern and northeastern sides. The coast faces the microtidal and wave-
113 dominated shore of Japan Sea (Ohshima and Yokota 1978). The tidal range is less than
114 0.6 m (Hydrographic and Oceanographic Department, Japan Coast Guard, 2004), the
115 mean significant wave height is 0.92 m (based on 2013 data), and the maximum
116 significant wave height is 7.32 m (based on 2004–2007 data) (Kawaguchi et al., 2015).
117 Strong westerly–northwesterly winds prevail, especially in winter (i.e., winter
118 monsoon), which approach orthogonally to the coast (Fig. 1). Figure 2 shows the
119 maximum and significant wave heights and the wave orientations observed in the bay
120 during the survey years. High waves were dominant in winter corresponding to the
121 strong wind, and their up-current orientations concentrated to northwest perpendicular
122 to the coastline (Fig. 2).
123 Highly deflected wave-influenced deltas should be considered as strand plains
124 especially when the major sediment input is externally (Bhattacharya and Giosan, 2003;
125 Bhattacharya, 2006). However, large volumes of the sediments along the Ishikari coast
126 are sourced internally (i.e., from the Ishikari River), and the coastline slightly protrudes
127 toward the river mouth. The low planform aspect ratio of deltas is probably controlled
128 by wave-angle climates (Ashton and Giosan, 2011) and a fluvial dominance ratio

(Nienhuis et al., 2015), which is defined as river sediment input with respect to the potential maximum alongshore sediment transport away from the river mouth. According to these theoretical studies, the Ishikari coast has dominant high-angle waves and low fluvial dominance ratio. We therefore treat the Ishikari coast as a deflected delta, which is an end member of wave-influenced delta geomorphology (e.g., Nienhuis et al., 2020).

The shore-normal wind-driven surface currents generate not only longshore currents, but also shore-parallel southwest oriented bottom currents in the Ishikari Bay because of Coriolis and Ekman effects. In addition, winds are stronger along the northeastern region of the coast than the southwestern region, and the resultant pressure gradient forces within the coastal water mass generate southwest oriented currents in the bay (Mizutani and Nakajima, 1997; Yamashita et al., 1999). The bottom currents were recorded in the zone of 15–30 m water depth by acoustic Doppler current profiler (Yamashita et al., 1998; 1999) (Fig. 3). Southwest directed strong bottom currents exceeding 0.4 m/s were widely observed in winter, while weak bottom currents directed northeast were dominant in summer.

The seafloor topography of the Ishikari coast is simple (Figs. 1 and 5). The bathymetric contours are parallel to the shoreline. The upper zone of the shoreface (≈4 m) dips at 1°, with slightly steeper gradients in local. The seafloor at water depths of 4–16 m dips at 0.3–0.4°, and the deeper areas have gradients lower than 0.1°. Longshore bars and troughs are formed at water depths of 2–6 m. A lobate mound is recognised at the front of the Ishikari River mouth, which is considered a modern subaqueous delta lobe (Ohshima et al., 1978). The plan-view morphology of the lobe slightly extends northward (Fig. 1). The modern sediments cover seafloor at water depths shallower than 40 m, whereas relict sediments are distributed at a depth deeper than 40 m (Ohshima and Yokota, 1978). According to Ohshima and Yokota (1978), the relict sediments consist of medium to coarse-grained clean sand (medians are 1–2 phi, and mud contents

156 are less than 5 wt%), that are significantly coarser than the modern lower shoreface
157 sands (medians are > 3 phi).

158 The Ishikari River has a length of 268 km (364 km before artificial linearisation of the
159 river course) and a drainage area of about 14×10^3 km^2. The average water discharge
160 based on the past 50 years is 15 km^3/year and the estimated sediment discharge is 2×10^6
161 t/year (Yamazaki and Yamashita, 2004). The Ishikari River is the only major river
162 entering Ishikari Bay. A large proportion of the coastal sediments is supplied from this
163 river (Ohshima and Yokota 1978; Suga and Hamada 2001), and about 80 % of the
164 annually discharged sediments are supplied in snowmelt season (Shimizu et al., 1998).
165 Suspended muddy sediments extend up to 50 km northward along the eastern margin of
166 the bay during the spring (Geological Survey of Hokkaido, 2003). Under fair weather
167 conditions in summer, a surface of the delta lobe is covered by muddy sediments at the
168 water depth deeper than 10 m (Suga and Hamada, 2001) (Fig. 1).

169 At the lower reaches, the Ishikari River has a single meandering channel that deflects
170 NE-ward parallel to the shoreline (Fig. 1). The channel is separated from the open ocean
171 by a river mouth spit with 10-m-high aeolian sand dunes (the Ishikari Sand Dune). The
172 location of the Ishikari River mouth had been migrating NE-ward with growth of the
173 spit and erosion of the downdrift (northeast) margin of the river mouth (Yamazaki and
174 Yamashita, 2004) (Fig. 4A). The growth rate of the spit during 1913–1976 was 17.8
175 m/year, as estimated by topographic maps and aerial photos (Arai, 1981). However, the
176 growth of the spit has been disrupted, and the river mouth stabilised since 1976 due to
177 revetment work at the downdrift margin of the river mouth (Yamazaki and Yamashita,
178 2004). Although the growth direction of the spit suggests net longshore sediment
179 transport NE-ward, several studies have suggested that foreshore sands are transported
180 both SW-ward (updriftward) and NE-ward (downdriftward) or predominantly SW-
181 ward. This is because drifted sands are predominantly trapped at the eastern side of the
182 artificial groin system (Ishikari Bay New Port: IBNP) (Fig. 4B, C) (Arai, 1981;

183 Yamashita et al., 2000; Suga and Hamada, 2001). The chronological change in the
184 coastline is further discussed in Section 4.3.
185
186 ## 3. Materials and Methods
187 *3.1. Sampling and grain-size measurement*
188 Along the Ishikari coast, a total 249 samples of seafloor sediments were collected
189 mainly along 28 transects, oriented perpendicular to the coastline, spaced mainly 500 m
190 or 1000 m apart (Fig. 5). Sampling surveys were performed in summer, June 1996,
191 September 1997, September 2004, August 2014, and August 2016. Most of the samples
192 on the updrift side of the Ishikari coast were collected in 1996–1997 by K. Suga and S.
193 Hamada (Suga and Hamada, 2001). The samples were collected in 2004 by K. Nishina
194 to complement the data obtained around the river mouth. We performed new sampling
195 surveys in 2014 and 2016 to collect offshore sediments from the downdrift area, from
196 the foreshore to the uppermost shoreface sands throughout the entire coast.
197 Oceanographic conditions (maximum and significant wave heights and wave
198 orientations) in the Ishikari coast during the sampling survey years 2014 and 2016 were
199 shown in Figure 2. There was an extremely limited number of significant storm events
200 before these surveys in the summer season. Even if samples were collected at different
201 dates, they are all representative of a summer period. This mix of dates has the
202 advantage to “filter” any short-term event which could have impact sediment
203 characteristics. Only long-term sediment behaviour (over 10 years) will be highlighted,
204 which is the aim of the present work.
205 Surface sediment samples (up to 2 cm depth) of the seafloor at water depths of 2–23 m
206 were collected using a Smith McIntyre grab sampler (1/20 m^2, Rigo Co., Ltd, Japan).
207 Along the coastline, sand samples in the foreshore and shallow water depth zone (≈1 m)
208 were collected at 100–500 m interval. The former was collected directly using a scoop
209 at up to 2 cm depth, while the latter was collected using PVC pipes up to 5-10 cm depth.
210 The seafloor sands around the mouth of the Ishikari River were collected at closer

intervals. The collected samples were prepared by chemical dissolution of organic matter and $CaCO_3$ using a 6% hydrogen peroxide solution and 20 vol.% acetic acid. Grain-size analysis was performed with a laser microgranulometer (Coulter counter LS230, Coulter Co., USA, 117 classes in size range 0.4 μm to 2 mm). Granules exceeding the measurement range were removed via sieving through -0.5 phi (1.41 mm) mesh before analysis. Few samples contained granules of ≈5 % weight. Statistical parameters, mean, sorting (standard deviation (σ)), and skewness, were calculated by the logarithmic method of moments using the GRADISTAT programme (Blott and Pye, 2001).

3.2. Grain-size trend analysis

The STA© (McLaren, 1981) was first introduced to interpret sediment transport directions along survey lines (i.e., one-dimensional approach). It is based on the comparison of three statistical parameters (mean, sorting and skewness) of grain-size distributions of sediment samples and their relative changes. As summarized in Kairytė and Stevens (2015), the main factors influencing grain-size composition of sediments are the: (i) winnowing; (ii) selective deposition of a portion of the grain-size distribution in transport; and (iii) total deposition. McLaren's model assumes that: (i) sediment in transport must be finer, better sorted and more negatively skewed than its source sediment (case: FB-); (ii) a lag must become coarser, better sorted and more positively skewed (case: CB+); and (iii) successive deposits may become finer or coarser, but the sorting must become better and skewness more negative or more positive with finer or coarser deposits, respectively (McLaren and Bowles, 1985; Kairytė and Stevens, 2015). Namely, the method assumes that the trends of FB- and CB+ have a higher frequency of occurrence in the direction of transport between two points.

Gao and Collins (1991) modified McLaren's method and provided a procedure for two-dimensional data treatment, in which each sample is compared with its nearest neighbours in any direction. Through this refinement, a two dimensional grain-size trend analysis (GSTA) is used as a qualifying method which defines trend vectors

(directions and patterns) based on the analysis of particular spatial relationships (trends) between the mean size, sorting and skewness of sediment samples (Poizot and Méar, 2010). Poizot et al. (2008) reviewed the Gao and Collins' approach and proposed a workflow to enhance the definition of trend pathways through the GSTA approach. One of the main proposals was the introduction of geostatistical tools to perform some pre-treatments allowing for a better choice of GSTA parameters. Most of the proposals were integrated in a GIS based software GiSedTrend (Poizot and Méar, 2010).

Before the analysis by GiSedTrend, the variographic analysis of the data set allows the characteristic distance (D_g) to be defined using GSTA computation and, the spatial variation model of the statistical parameters (mean, sorting and skewness) to be defined. The spatial models are then used to produce interpolation maps (Fig. 6) from which a regular grid is extracted for each parameter. In the present study, a 200 m grid spacing was defined. These grids were then at the inlet of the GSTA approach. The variographic analysis and interpolation operations were performed under R Statistical language (R Core Team, 2020) using the geostatistical package R Geostats (Renard et al., 2020). The CircStats R package (Lund and Agostinelli, 2018) provided the circular statistics used to compare trend case directions.

Following the above, three different GSTA analysis were performed using GiSedTrend: a) the classical combined cases CB+ and FB-; b) FB- case alone; and c) CB+ case alone. Results of the two latter trend cases were used to compare their relative impacts to the combined trend case of CB+ and FB-. Some barriers (linear objects) created to represent the coast and seawalls were considered during the GSTA computation. The semi-variogram analysis (Matheron, 1973) of the interpolated dataset showed that the distance where the model first flattened out (i.e., the range) ranged from 3200 m to 4000 m. These distances represent the spatial scale at which samples are considered as neighbors (correlated). Therefore, characteristic distance (D_g) was defined at 4000 m in the analysis, which is the highest distance between all the parameters.

4. Results

4.1. General grain-size characteristics

The modern seafloor sands in the Ishikari coast mainly consisted of medium- to very fine-grained sands of poorly- to very poorly sorted and very fine-skewed grain-size characteristics (Fig. 7). The maximum mud content of the samples was 70% (Figs. 5 and 7); these sands showed a simple fining trend as water depth increased (Fig. 7), a typical sediments behaviour in wave-dominated coasts (Reading and Collinson, 1996). Muddy sediments exhibited a focused distribution at relatively shallow depths in front of the Ishikari River mouth during spring and summer, which were covering the delta lobe (blue circles in Fig. 5). The samples of mode phi>4 were excluded from the analysis, since sand movements are considered to be expressed under no cohesive conditions, whereas muddier sediments are considered to move under cohesive conditions.

Based on the grain-size parameters, four depth zones were defined: foreshore zone, uppermost shoreface zone (water depth: ≈2 m), upper shoreface zone (water depth: 2–8 m), and lower shoreface zone (water depth: 8–23 m) (Fig. 7). The foreshore sands showed coarser mode grain-sizes of 0.5–2.0 phi (mean phi: 0.5–2.3) and were classified as poorly sorted sands ($1.0<\sigma<2.0$), although they were better sorted than the shoreface sands (Fig. 7B, C, D). The uppermost shoreface sands were also coarse (mode phi: 0.5–2.0) but showed a wider range of mean grain sizes (0.5–3.3 phi) than foreshore sands and were classified as poorly sorted to very poorly sorted ($0.7<\sigma<3.4$). The mode grain size of the upper and lower shoreface sands generally ranged 1.6–3.6 phi (mean phi: 0.6–5.6). The upper shoreface sands showed a clear fining trend to deeper waters, but the sand in the lower shoreface had a small range grain size variation (Fig. 7B, C, D).

Skewness of the foreshore and the uppermost shoreface sands showed greater variabilities, from symmetrical to very fine skewed (-0.4–8.0), whereas the sands of the upper and lower shoreface were very fine skewed (1.0–4.0) (Fig. 7E). In terms of

kurtosis, most of the analysed sands were classified as leptokurtic to very leptokurtic (Fig. 7F). On the scatter plot of mean vs. skewness, most of the samples negatively correlated, however, 12 samples from foreshore and uppermost shoreface deviated from this trend (Fig. 8 and supplement table). These sediment samples were excluded from the GSTA analysis.

Interpolation maps of these grain-size parameters (mean, sorting and skewness) suggest there are interrelationships among these parameters (Fig. 6).

4.2. Spatial variation of grain-size parameters and grain-size trends

The spatial variation of the grain-size parameters suggested several trends, both perpendicular and parallel to the coastline (Figs. 6 and 9). The foreshore–upper shoreface sands had the coarsest grain size neighbour at the Ishikari River mouth. With increasing distance from the river mouth, the grain size of the nearshore sands became finer both along-shore and cross-shore, exhibiting the highest gradients around the river mouth (Figs. 6 and 9). Along the offshore dike of Ishikari Bay New Port (IBNP), the shore-parallel gradient became unclear. In the western side of IBNP, westward fining then coarsening trend appeared with a lesser intensity than the eastern side of IBNP (Figs. 6 and 9).

The results of GSTA (Fig. 10) showed that systematic trend fields of CB+ existed within a wide area with the high degree of confidence (i.e., long vectors). The vector fields of the FB- trend case appeared very locally (Fig. 10). The combined CB+ & FB- case exhibited the same main direction characteristics as the single CB+ trend case. The directions shown in the wind roses, Figure 10 (right column), demonstrate that there was little difference between the CB+ and CB+ & FB- trend cases. This indicates that the CB+ trend provides the most significant information in the CB+ & FB- combined trend case. Namely, the CB+ is the dominant trend case in the Ishikari coast. The vector field CB+ was widely distributed, except in the nearshore zones (i.e., foreshore and uppermost shoreface zones). The wind rose of the CB+ trend (Fig. 10, top right) shows

a globally southward vector direction (159.3° of mean direction). Two directions sustain a higher number of vectors around the mean direction: SW-ward and SE-ward.

Despite the general trends highlighted in Figure 10 by analysis of the statistical parameters, the CB+ trend vector field showed a more complex behaviour. According to the vector field, three different sectors can be recognised each corresponding to one-third of the studied area (Fig. 11). In the eastern sector centred on the river mouth (*sector A* on Fig. 11), the trajectory of CB+ vectors draw a clockwise rotation in the downdrift area, and an anti-clockwise rotation in the updrift area. These vectors converge to the head of the spit at approximately 2000 m southwest (updrift side) of the river mouth (Fig. 11). A small area in the sector, containing some FB- trend vectors (~30 vectors) oriented mainly SW-ward, is highlighted offshore (Fig. 10). The second sector is centred on the IBNP (*sector B* on Fig. 11). CB+ trend vectors separate in two directions at the tip of the outermost dike. Vectors located northeast of sector B turn southward to concentrate 1 km north of IBNP. The other vectors turn gently from SW-ward to southward near the dike. FB- trend vectors are present at two locations in this sector, offshore with an eastward direction, and at the southern part of the sector with a NE-ward direction (Fig. 10). The last sector starts, in the north, approximately 1 km south of IBNP and ends at the southwestern side of the studied area (*sector C* on Fig. 11). In this sector, CB+ vectors show divergent paths start radially from the centre to the E, ESE, S, SW, and W. North of this sector, CB+ trend vectors highlight a SE to East-ward direction pointing to IBNP south inlet. In the south part of sector C, general vector direction oriented southward in the offshore zone, which turned SW-ward as they approached the coast. Some westward directed FB- trend vectors are present near the coast at the Shinkawa river mouth (Fig. 10).

4.3. Interpretation of sediment pathway

The CB+ vector fields appeared globally in the lower shoreface zone. In sector A and the northeastern part of sector B, the onshore directed CB+ trends predominant in the shallower part of the lower shoreface reflect a spatial gradient in the degree of

winnowing of fine fractions controlled by water depth. The trend oriented perpendicular to the bathymetric contour lines corresponds directly with the shoring storm waves and/or the wind-driven surface currents. Bathymetric lines from -20 m to -3 m are parallel to the coast and have a concave shape toward offshore. Because of refraction on the seafloor, storm waves align progressively to the general bottom morphology. In sector A, the onshore directed CB+ vectors converging to the head of the river mouth spit (at the point approximately 2000 m southwest from the mouth) reflects combined effects of the river sediment discharge and storm waves concentrated at the river mouth due to bottom refraction on the delta lobe.

In the deeper zone of the lower shoreface, the CB+ trend wind rose graphic (Fig. 10, top right) shows a globally SW-ward vector direction. The trend vectors correspond with the decrease in mud content rather than the composition of sand fractions (Figs. 9 and 12). This SW-ward trend is parallel to the bathymetric contour lines and well concordant with the orientation of strong bottom currents observed in the Ishikari Bay (Mizutani and Nakajima, 1997; Yamashita et al., 1998; 1999). Thus, it is considered that the lower shoreface sands have been re-deposited successively with progressive mud winnowing by the bottom currents. Such behaviour is reinforced in sector B with the presence of IBNP. At this location, the offshore dike divides the bottom currents transport trend in two directions, SE-ward and SW-ward (Fig. 11, sector B). The deflection of the bottom currents on the offshore side of the dike deviates sediment transport to a westward direction. The meeting of the deflected currents on the dike with the offshore currents causes a decrease in current particle transport. Very small size CB+ trend vectors at this location show that the trend has less confidence.

In sector C, an eastward CB+ trend appeared in the lower to upper shoreface zone at its NE part. The trend is disharmonic with the global trend in the bay, and the origin of the trend is uncertain. The trend reflects a decrease in mud content (Fig. 9). The finer sediments are distributed at the front of the Shinkawa river (canal) mouth, and the trend

could have been affected by mud deposition discharged from the river during snowmelt season.

Also, the FB- trend is shown in the wind rose (Fig. 10, bottom right). The trend shows that two main opposite directions are present and are globally parallel to the coastline. This behaviour is related to the alternative tide currents in the bay. The statistical confidence for the vectors (the length) is not high, meaning the tide currents have a small data set footprint that is, they do not provide enough energy to clearly impact the sediment characteristics.

Due to the greater variability in skewness, GSTA revealed no apparent trend field in the nearshore zone. This indicates that the grain-size composition of nearshore sands is affected by numerous forces in the nearshore zone. However, the gradual fining of sand fractions along the coastline, and the chronologic transition of the coastlines suggest that longshore current is the dominant force. The symmetric fining trend of the nearshore sands away from the Ishikari River mouth (sector A and northeastern part of sector B), mostly reflect the sand-size fraction composition rather than the mud content (Figs. 9 and 12). Such trends have also been recognised in the previous studies conducted before the construction of IBNP (Taishi, 1977; Arai, 1981). This trend indicates both a longer updriftward and downdriftward transport of finer-grained sand fractions away from the river mouth by longshore currents, whereas coarser-grained fractions remain along the head of spit, as lag deposits. Field experiment carried out in 1969 supports this interpretation. In the experiment, fluorescent colouring sands were added to the water at depth of 0 m (beach), 3m, and 5m at the centre of the coast (7 km southwest of the river mouth). These sands were transported south-westward (updrift) during summer, but migrated both southwest- and northeast-ward in winter, resulting in net nearshore sand transport directed south-westward (updrift) (Kougami et al., 1971).

The transition of the coastline between 1947-1971 (before IBNP construction, i.e., under natural conditions) suggests accreted sand was distributed almost evenly to both

the updrift and downdrift sides, with a slight preference toward the downdrift-side (updrift:downdrift=44:56) (Fig. 4). Yamashita et al. (2000) evaluated the volume of accreted coastal sands on the updrift-side from a depth of -12 m underwater to 4 m above mean sea level during 1947–1976, and estimated that approximately 20×10^4 m^3 sands was accreted annually. This volume was two-thirds of the annually discharged sands (approximately 30×10^4 m^3/y) from the Ishikari River. After the construction of IBNP, the sand transported updriftward was trapped by the eastern side of IBNP (Fig. 4B, 4C). Fukuda et al. (2016) estimated the volume of sands trapped annually was 23×10^4 m^3/y from 2011–2015, and concluded that most of the sand fractions transported updriftward were accreted there. In contrast, the coastline has regressed at average rate of 0.44 m/y on the western side of IBNP (Fig. 4C). This suggests that sand starvation on the western side of IBNP is due to the interception of sand transport along the shoreline. These results also imply that sediment input from onshore-ward sediment transport by waves is insufficient to sustain or grow the coastline in this area.

The remaining sand sourced from the river was deposited around the tip of the spit on the downdrift side of the delta, and in the offshore area. However, the growth of the spit has been restrained in recent decades due to a revetment that was constructed simultaneously with IBNP. On the downdrift side of the delta, the groin protruding from the revetment has disrupted the downdriftward sediment transport from the river mouth, therefore, leading to a significant reduction in sand accretion on the downdrift side.

5. Discussion

In delta system, driving forces of sediment distribution, such as waves, tide, and river inflows, are generally complex. In addition, conditions often drastically change with the season (Davis, 1985; Reading and Collinson, 1996). Although the GSTA approach highlights that the resultant grain-size trend is generated by the most influential trend case or by combined effect of other factors. It underlines the strengths of studying trend

cases separately, as it enables better identification of environmental processes responsible for spatial and quantitative sediment distribution. In this study, the dataset used in the GSTA was composed of sediment samples obtained at different dates over the years but always in the same season (summer). This acts as a time averaging filter, avoiding “noise” which can be induced by non-recurrent or erratic events that may not be recognized as "noise" from a single dataset. This allows for the general mean processes acting on sediment sorting to be identified. In the same manner, working at the scale of the Ishikari Bay, general spatial processes are apparent in the dataset. Although it is possible that natural or human activity may change the sediment dynamics (e.g. Anthony, 2015; Nienhuis et al., 2020) and resultant grain size parameters of the seafloor sediments over many years, the variograms show that the granulometric parameters of seafloor sediments collected in different years have a good spatial autocorrelation and can be considered for trend analysis. In detail, the geostatistical analysis performed prior to the GSTA provided variograms of the three statistical parameters showing sills. This is an indication of the presence of autocorrelations over the parameters (Journel and Huijbregts, 1976; Wackernagel, 1988), that is, the action of one or multiple processes is highlighted. Consequently, the characteristic distance defined during the variographic analysis is linked to the main processes and the GSTA results show their spatial organisation.

As the CB+ trend is recognised as the dominant trend on the Ishikari coast, it can be concluded that this trend is mainly related to energetic transport processes of winter storm waves. In sector A, onshore CB+ vectors converging from the lower shoreface zone to the head of river mouth spit reflects the combined effects of the river sediment discharge and the winnowing of fine fractions controlled by water depth. Although a similar trend was observed in the Rhône Delta, France using the GSTA approach (Maillet et al., 2011), such behaviour was interpreted as a consequence of the swell action which keeps most of fine fractions out of river mouth. Meanwhile, swells do not

develop in the Japan Sea (Sugimoto and Chikasawa, 2008), and therefore, the winnowing of the nearshore sediments are mainly driven by storm waves in the case of Ishikari coast.

In the offshore zone, the seafloor sediments have been successively re-deposited to the southwest by the bottom currents, with progressive mud winnowing. In other words, the subaqueous delta front deposits coarsen to the updrift side corresponding with the true downcurrent direction. The southwest-ward bottom currents in the bay are generated by strong north westerly winds during winter storms. The wind-driven, on-shore directed, surface currents deviate southwest-ward above the seafloor of the lower shoreface by Coriolis and Ekman spiral effects (Fig. 3). These processes have been confirmed by a numerical study (Le et al., 2006). The footprint of the winter bottom currents persists until summer, as the transport processes in the summer season, driven by calm waves, cannot sufficiently modify the winter inherited sediment organization.

Although the net longshore sediment transport direction of the entire system remains uncertain, nearshore sands are transported updriftward on the updrift-side of the delta, especially during summer. It is generally considered that the growth of an asymmetric and deflected delta requires dominant sediment accretion in the updrift side under a downdriftward net longshore sediment transport condition. To explain this, external sediment sources are often identified as the contributors to the enhanced updrift area (Reading and Collinson, 1996; Bhattacharya and Giosan, 2003; Bhattacharya, 2006; 2010; Anthony, 2015). However, there are no major rivers nor sea-cliffs in the west of Ishikari coast which can provide significant volume of sands. Therefore, it is considered that the updriftward net longshore transport of the internally sourced sediments has been sustaining the growth of the updrift side of the Ishikari delta (Fig. 13). Sediment delivery patterns in the offshore zone are thought to have less influence on the planform of deltas (Bhattacharya and Giosan, 2003; Ayranci and Dashtgard, 2016). Therefore, the predominant updriftward sediment transport in the lower shoreface zone is not

surprising. However, sands covering the lower shoreface may enhance the progradation of the delta-front on the updrift-side.

The cause of the northeast advance of the river mouth spit under the updriftward sediment transport condition along the shoreline is still uncertain; however, it can most likely be explained by the slightly oblique angle at which the waves approach the river mouth. Such waves typically form swash bars and subaqueous levees on the updrift side (Wright, 1977; Giosan, 2007), and can directly deflect river mouth jets (Nardin and Fagherazzi, 2012; Nienhuis et al., 2016). Such processes occur in winter at the Ishikari River mouth, since the river discharge is significantly smaller during winter. Once a river course is deflected, the processes are enhanced and long-lasting, until spit breaching occurs due to river currents that favour spit elongation/accretion on the updrift side and erosion on the coast downdriftward from the river mouth. To further understand the correlation between delta growth and sediment dynamics and validate the conclusions of the present study, detailed modelling of the growth of the deflected delta under with an internal sediment source will be required.

6. Conclusion

Sedimentological analysis and grain-size trend analysis (GSTA) of seafloor sediments along with other observational data, revealed dominant updriftward sediment transport on the updrift-side of a deflected delta system:

(1) Coarser, better-sorted, and more positively skewed (CB+) trends are dominant on the Ishikari coast, this is mainly due to energetic sediment transport processes driven by winter storm waves.

(2) The updriftward CB+ trends of the lower shoreface sands are caused by strong bottom currents in the coast during winter storms, showing successive re-deposition of seafloor sands with progressive mud winnowing.

(3) Gradual fining of foreshore sands, and the chronological transition of the coastline after the construction of large a port suggest that longshore sediment transport also

directs updriftward on the updrift side of the Ishikari delta.

(4) The growth of deflected deltas depends on dominant sediment accretion on the updrift-side. Thus, the dominant updriftward sediment transport condition on the updrift side can be rationalised in the case of internally-sourced deflected deltas.

(5) The deflection of the Ishikari delta planform can most likely be explained by deflected mouth bars and river mouth jets due to the slightly oblique angle at which waves approach the river mouth. Consequently, the deflection of the Ishikari delta is probably independent of the direction of dominant sediment transport.

Acknowledgments

We thank K. Suga and S. Hamada for providing seafloor sand samples. The manuscript was greatly improved by the suggestions by Toru Tamura, two anonymous reviewers, and Edward Anthony (Editor-in-Chief). This study was supported in part by Grant-in-Aid for Scientific Research from the Ministry of Education, Science and Culture of Japan (No. 26350480).

References

Ainsworth, R.B., Vakarelov, B.K., MacEachern, J.A., Nanson, R.A., Lane, T.I. Rarity, F., Dashtgard, S.E., 2016. Prosess-driven architectural variability in mouth-bar deposits: a case study from a mixed-process mouth-bar complex, Drumheller, Alberta, Canada. Journal of Sedimentary Research, 86, 512–541. https://dx.doi.org/10.2110/jsr.2016.23

Anthony, E.J., 2015, Wave influence in the construction, shaping and destruction of river deltas: A review. Marine Geology, 361, 53–78. https://dx.doi.org/10.1016/j.margeo.2014.12.004

Ashton, A.D. and Giosan, L., 2011, Wave-angle control of delta evolution. Geophysical Research Letters, 38, L13405. https://doi.org/10.1029/2011GL047630

Asselman, N., 1999. Grain-size trends used to assess the effective discharge for floodplain sedimentation, river Waal, The Netherlands. Journal of Sedimentary Research, 69, 51–61. https://doi.org/10.2110/jsr.69.51

Ayranci, K., Dashtgard, S.E., 2016. Asymmetrical deltas below wave base: insights from the Fraser

River delta, Canada. Sedimentology, 63, 761–779. https://doi.org/10.1111/sed.12237

Arai, K., 1981. Effects of the construction of Ishikari Bay New Port on shoreline and foreshore sediments, Hokkaido, Japan. Journal of Graduate School of Environmental Science, Hokkaido University, 4, 149–159. (in Japanese)

Bhattacharya, J. P., 2006. Deltas. In: Posamentier, H. W. and Walker, R. G. (Eds.), Facies models revisited, pp. 237–292. SEPM Special publication no. 84, Tulsa, Oklahoma.

Bhattacharya, J. P., 2010. Deltas. In: James, N. P. and Dalrymple, R. W. (Eds.), Facies Models 4, pp. 233–264. Geological Association of Canada GEOtext 6.

Bhattacharya, J. P., Giosan, L., 2003. Wave-influenced deltas: geomorphological implications for facies reconstruction. Sedimentology 50, 187–210. https://doi.org/10.1046/j.1365-3091.2003.00545.x

Blott, S.J., Pye, K., 2001. GARDISTAT: a grain size distribution and statistics package for the analysis of unconsolidated sediments. Earth Surface Processes and Landforms 26, 1237–1248. https://doi.org/10.1002/esp.261

Carriquiry, J., Sánchez, A., 1999. Sedimentation in the Colorado river delta and upper gulf of California after nearly a century of discharge loss. Marine Geology, 158, 125–145. https://doi.org/10.1016/S0025-3227(98)00189-3

Carriquiry, J., Sánchez, A., Camacho-Ibar, V., 2001. Sedimentation in the northern gulf of California after cessation of the Colorado river discharge. Sedimentary Geology, 144, 37–62. https://doi.org/10.1016/S0037-0738(01)00134-8

Davis, R.A. Jr. ed., 1985. Coastal Sedimentary Environments. Springer-Verlag, New York, Berlin, Heidelberg, Tokyo, 716p.

Dominguez, J.M.L., 1996. The São Francisco strandplain: a paradigm for wave-dominated deltas?. In: De Baptist, M. and Jacobs, P. (Eds.), Geology of Siliciclastic Shelf Seas, Geological Society of London Special Publication, 117, 217–231. https://doi.org/10.1144/GSL.SP.1996.117.01.13

Fukuda, S., Yatsuyanagi, A., Yokoyama, S., 2016. Drifted sands dynamics and countermeasures on the site of Ishikari Bay New Port. Proceedings for the 60th technical workshop of Hokkaido Regional Development Bureau. https://thesis.ceri.go.jp/db/documents/public_detail/62320/ (in Japanese)

Gao, S., Collins, M., 1991. A critique of the ‘‘Mc Laren method’’ for defining sediment transport paths-discussion. Journal of Sedimentary Petrology, 61, 143–146.

https://doi.org/10.1306/D42676A9-2B26-11D7-8648000102C1865D

Gao, S., Collins, M., Lanckneus, J., De Moor, G., Van Lancker, V., 1994. Grain size trends associated with net sediment transport patterns: an example from the Belgian continental shelf. Marine Geology, 121, 171–185. https://doi.org/10.1016/0025-3227(94)90029-9.

Geological Survey of Hokkaido, 2003. Geological Map of the Coastal Area of Hokkaido -3- Northern part of Sea of Japan. Scale 1:200,000. Geological Survey of Hokkaido, Sapporo. (in Japanese with English abstract)

Geological Survey of Hokkaido, 2004. The dynamics of plant pieces as part of the environmental creation project suitable for useful fishery resources at around the mouth of the Ishikari River. Geological Survey of Hokkaido, Sapporo, 54 p. (in Japanese)

Giosan, L., 2007, Morphodynamic feedbacks on deltaic coasts: Lessons from the wave-dominated Danube Delta. In: Kraus, N. C. and Rosati, J. D. (Eds.), Coastal Sediments '07, pp. 828–841, https://doi.org/10.1061/40926(239)63

Hasegawa, H., 1982. Depositional environments of sandy sediments of the Ishikari coastal plain. Geographical Review of Japan, 55, 75–84. https://doi.org/10.4157/grj.55.75 (in Japanese with English abstract)

Hydrographic and Oceanographic Department, Japan Coast Guard, 2004. 2004 Tide tables, Japan and its vicinities. Bibliography of Japan Coast Guard No. 781. (in Japanese)

Journel, A G, Huijbregts, C J. 1976. Mining geostatistics. Academic Press, London, 600p.

Kairytė, M., Stevens, R.L., 2015. Composite methodology for interpreting sediment transport pathways from spatial trends in grain size: A case study of the Lithuanian coast. Sedimentology 62, 681–696. https://doi.org/10.1111/sed.12156

Kawaguchi, K., Inomata, T., Seki, K., Fujiki, T., 2015. Annual Report on Nationwide Ocean Wave Information Network for Ports and Harbors (NOWPHAS 2013). Technical Note of the Port and Airport Research Institute, no. 1305, 121p. (in Japanese with English abstract)

Kougami, Y., Osanai, G., Hoshi, F., Takamatsu, M., 1971, Drift sand along the Ishikari Coast. Proceedings of the Japanese Conference on Coastal Engineering, 18, 405–409. https://doi.org/10.2208/proce1970.18.405

Le, V.S., Yamashita, T., Miyatake, M., Shinohara, R., 2006. Characteristics of winter current pattern in the Ishikari Bay. Ann. Journal of Hydraulic Engineering, JSCE 50, 145–150. https://doi.org/10.2208/prohe.50.145

603 Lund, U., Agostinelli, C., 2018. CircStats: Circular Statistics, from "Topics in Circular Statistics"
604 (2001). R package version 0.2-6. https://CRAN.R-project.org/package=CircStats
605 Maillet, G. M., Poizot, E., Sabatier, F., Vella, C., Méar, Y., 2011. Pattern of sediment transport in a
606 microtidal river mouth using geostatistical sediment-trend analysis. Journal of Sedimentary
607 Research, 81, 138–152. https://doi.org/10.2110/jsr.2011.8
608 Matheron, G., 1973. The intrinsic random functions and their applications. Advances in Applied
609 Probability, 5:439-468.
610 Matsushita, K., 1979. Buried landforms and the Upper Pleistocene–Holocene deposits of the Ishikari
611 coastal plain, Hokkaidō, North Japan. The Quaternary Research, 18, 69–78.
612 https://doi.org/10.4116/jaqua.18.69 (in Japanese with English abstract)
613 McLaren, P., 1981. An interpretation of trends in grain size measures. Journal of Sedimentary
614 Petrology, 51, 611–624. https://doi.org/10.1306/212F7CF2-2B24-11D7-8648000102C1865D
615 Mc Laren, P., Bowles, D., 1985. The effects of sediment transport on grain-size distribution. Journal
616 of Sedimentary Petrology, 55, 457–470. https://doi.org/10.1306/212F86FC-2B24-11D7-
617 8648000102C1865D
618 Mizutani, N., Nakajima, H., 1997. Characteristics of coastal currents in the Ishikari Bay. Proceedings
619 of Coastal Engineering, Japan Society of Civil Engineers, 44, 366–370.
620 https://doi.org/10.2208/proce1989.44.366 (in Japanese)
621 Nardin, W., and S. Fagherazzi, 2012, The effect of wind waves on the development of river mouth
622 bars. Geophysical Research Letters, 39, L12607. https://doi.org/10.1029/2012GL051788
623 Nienhuis, J. H., Ashton, A. D., Edmonds, D. A., Hoitink, A. J., F., Kettner, A. J., Rowland, J. C. and
624 Törnqvist, T. E., 2020, Global-scale human impact on delta morphology has led to net land area
625 gain. Nature, 577, 514–518. https://doi.org/10.1038/s41586-019-1905-9
626 Nienhuis, J. H., Ashton, A. D. and Giosan, L., 2015, What makes a delta wave-dominated? Geology,
627 43, 511–514. https://doi.org/10.1130/G36518.1
628 Nienhuis, J. H., Ashton, A. D., Nardin, W., Fagherazzi, S. and Giosan, L., 2016, Alongshore
629 sediment bypassing as a control on river mouth morphology. Journal of Geophysical Research,
630 Earth Surface, 121, 664–683. https://doi.org/10.1002/2015JF003780
631 Ohshima, K., Yokota, S., 1978. Sediments of Ishikari bay in Hokkaido. Bulletin of the Geological
632 Survey of Japan, 29, 501–529. (in Japanese with English abstract)
633 Ohshima, K. Ikeda, K., Yamaya, M., 1978. Topography of the Ishikari bay and lowland area.

Bulletin of the Geological Survey of Japan, 29, 461–476. (in Japanese with English abstract)

Poizot, E., Anfuso, G., Méar, Y., Bellido, C., 2013. Confirmation of beach accretion by grain-size trend analysis: Camposoto beach, Cádiz, SW Spain. Geo-Marine Letters, 33, 263–272. https://doi.org/10.1007/s00367-013-0325-3

Poizot, E., Méar, Y., 2010. Using a GIS to enhance grain size trend analysis. Environmental Modelling & Software, 25, 513–525. https://doi.org/10.1016/j.envsoft.2009.10.002

Poizot, E.; Méar, Y., Biscara, L., 2008. Sediment Trend Analysis through the variation of granulometric parameters: A review of theories and applications. Earth-Science Reviews, 86, 15–41. https://doi.org/10.1016/j.earscirev.2007.07.004

R Core Team, 2020. R: A Language and Environment for Statistical Computing.

Reading, H.G., Collinson, J.D., 1996. Clastic coasts. In: Reading, H. G. (Ed), Sedimentary environments: processes, facies and stratigraphy, 3rd edition. Blackwell Science, Oxford, 154–231.

Renard, D.; Bez, N.; Desassis, N.; Beucher, H.; Ors, F., Freulon, X., 2020. RGeostats, Geostatistical Package version 11.1.1.

Ríos, F., Cisternas, M., Le Roux, J., Corréa, I., 2002. Seasonal sediment transport pathways in Lirquen Harbour, Chile, as inferred from grain-size trends. Investigaciones Marinas. Valparaiso, 30, 3–23.

Rodriguez, A. B., Hamilton, M. D., Anderson, J. B., 2000. Facies and evolution of the modern Brazos delta, Texas: wave versus flood influence. Journal of Sedimentary Research, 70, 283–295. https://doi.org/10.1306/2DC40911-0E47-11D7-8643000102C1865D

Shimizu, Y., Saga, H., Hayakawa, H., Shinagawa, M., 1998. A study on sediment runoff of the Ishikari River. Annual Journal of Hydraulic Engineering, 42, 1039–1044. https://doi.org/10.2208/prohe.42.1039 (in Japanese)

Suga, K., Hamada, S., 2001. Littoral sediments and coastal erosion on the head of Ishikari Bay, Hokkaido. Report of the Geological Survey of Hokkaido, 72, 31–71. (in Japanese with English abstract)

Sugimoto, S., Chikasawa, M., 2008. A study on Japanese coastal wave characteristics using coastal wave observation by Japan Meteorological Agency. Weather service bulletin, 75, Spec. Issue S77 –S95. (in Japanese)

Taishi, H., 1977. Environmental distinction of sandy sediments and depositional environment in

sandy area of the Ishikari coast, Hokkaido, Japan. Geophys. Bulletin of Hokkaido University, 36, 1–15. (in Japanese with English abstract)

Wackernagel, H., 1988. Geostatistical techniques for interpreting multivariate spatial information. In: Chung, C.F., Fabbri, A.G. and Sinding-Larsen, R. (Eds.), Quantitative Analysis of Mineral and Energy Resources, pp. 393–409, NATO ASI Series C 223, Reidel Publishing Company, Dordrecht, Hollande. https://doi.org/10.1007/978-94-009-4029-1_24

Wright, L. D., 1977, Sediment transport and deposition at river mouths: a synthesis. Geological Society of America Bulletin, 88, 857–868. https://doi.org/10.1130/0016-7606(1977)88<857:STADAR>2.0.CO;2

Yamashita, T., Hoshi, H., Niiyama, M., Hasebe, T., Fukumoto, T., Tada, A., 1999. Three-dimensional characteristics of coastal currents in the Ishikari Bay in winter season. Proceedings of Coastal Engineering, the Japan Society of Civil Engineers, 46, 426–430. https://doi.org/10.2208/proce1989.46.426 (in Japanese)

Yamashita, T., Kinoshita, H., Hoshi, H., Narumi, H., Hashimoto, T., Fukumoto, T., Tada, A., 1998. Three-dimensional characteristics of coastal currents around the Ishikari Bay New Port. Proceedings of Coastal Engineering, the Japan Society of Civil Engineers, 45, 391–395. https://doi.org/10.2208/proce1989.45.391 (in Japanese)

Yamashita, T., Niiyama, M., Suganuma, T., Hayakawa, T., 2000. Characteristics of deposition and budget of discharged sediment from Ishikari River mouth in coastal region. Proceedings of Coastal Engineering, the Japan Society of Civil Engineers, 47, 676–680. https://doi.org/10.2208/proce1989.47.676 (in Japanese)

Yamazaki, S., Yamashita, T., 2004. Long-term fluctuations in outflow of suspended sediment from the Ishikari River and its sedimentation features in coastal area. Monthly Report, Civil Engineering Research Institute of Hokkaido, no. 617, 2–16. (in Japanese with English abstract)

690

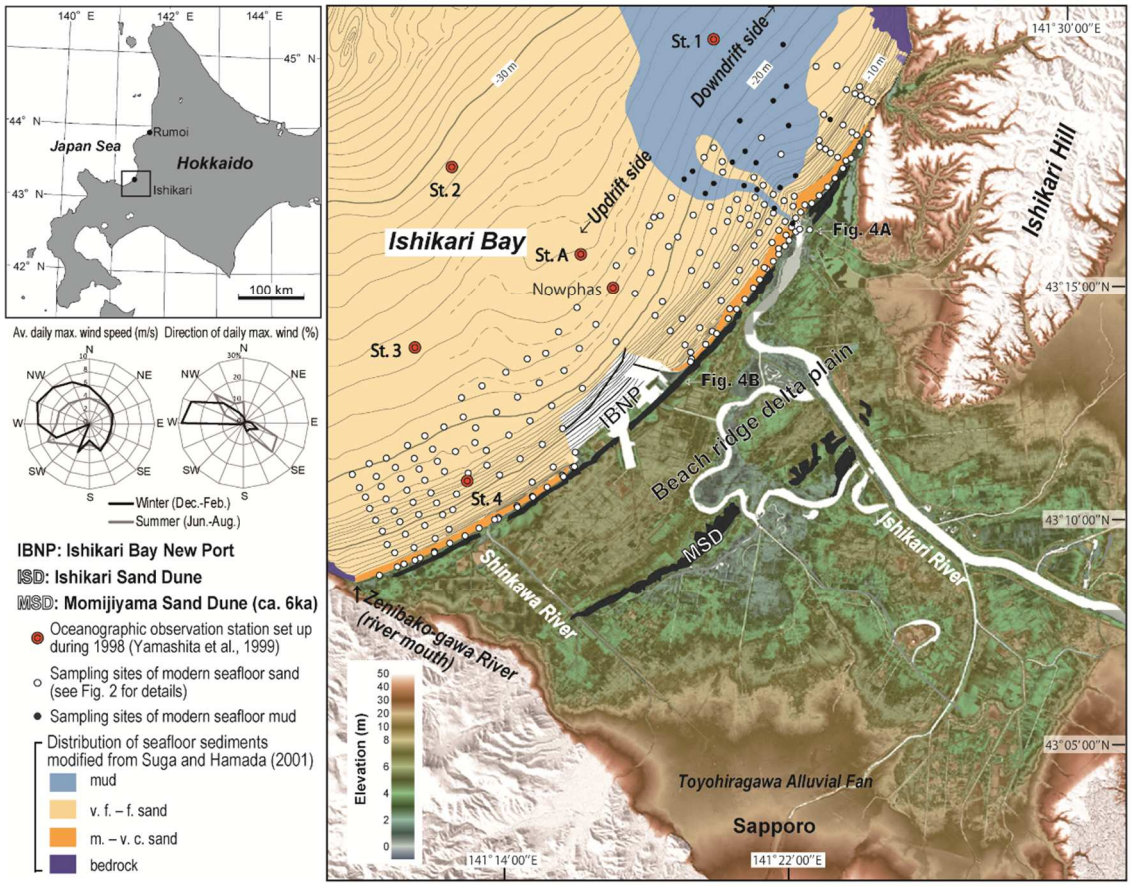

691

692 Fig. 1 Geographical map of the Ishikari Delta and the distribution of seafloor sediments in
693 Ishikari Bay. Radar charts show wind speed and direction of daily maximum wind from 1990
694 to 2017 in Ishikari Meteorological Observatory (Japan Meteorological Agency). The delta
695 plain consists mainly of beach ridge sands. The present Ishikari River mouth is located
696 near the northeastern margin of the coastline, showing a highly deflected planform. The
697 left bank of the lower reaches of the Ishikari River is barriered by a river mouth spit. The
698 digital elevation model is provided by the Geospatial Information Authority of Japan. The
699 bathymetric contour lines are based on the “Digital Topography of Ocean Floor M7000
700 Series” published by the Japan Hydraulic Association.

701

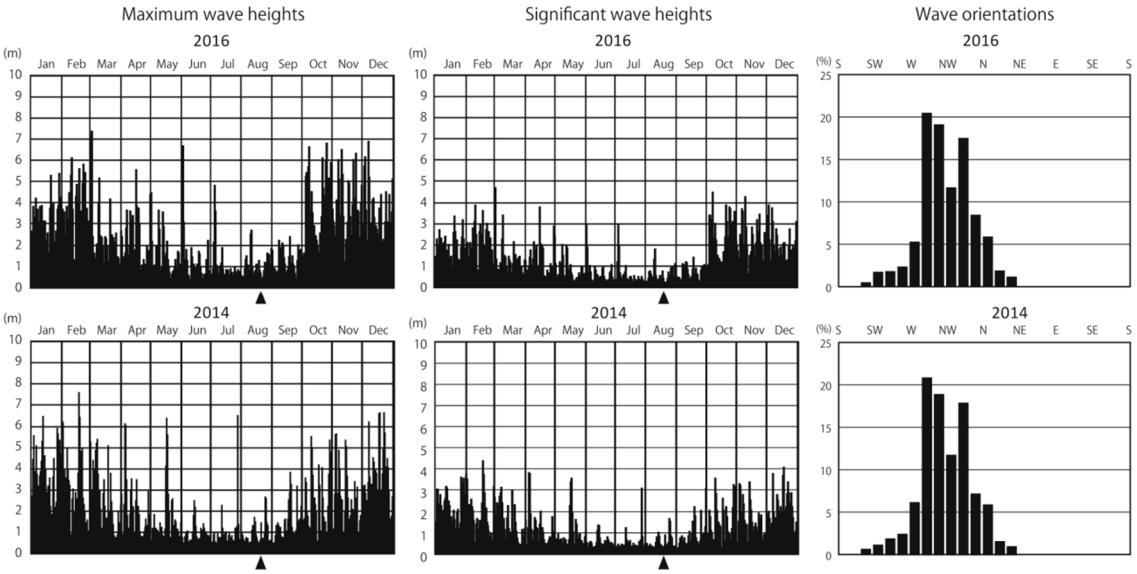

Fig. 2 Maximum and significant wave heights and wave orientations (up-current) in the Ishikari coast during the survey years 2014 and 2016. The data are based on the 2 hours interval observation data of Nationwide Ocean Wave Information Network for Ports and Harbours (NOWPHAS) system provided by the Ministry of Land, Infrastructure, Transport and Tourism in Japan (data are available online at https://www.mlit.go.jp/kowan/nowphas/index eng.html).

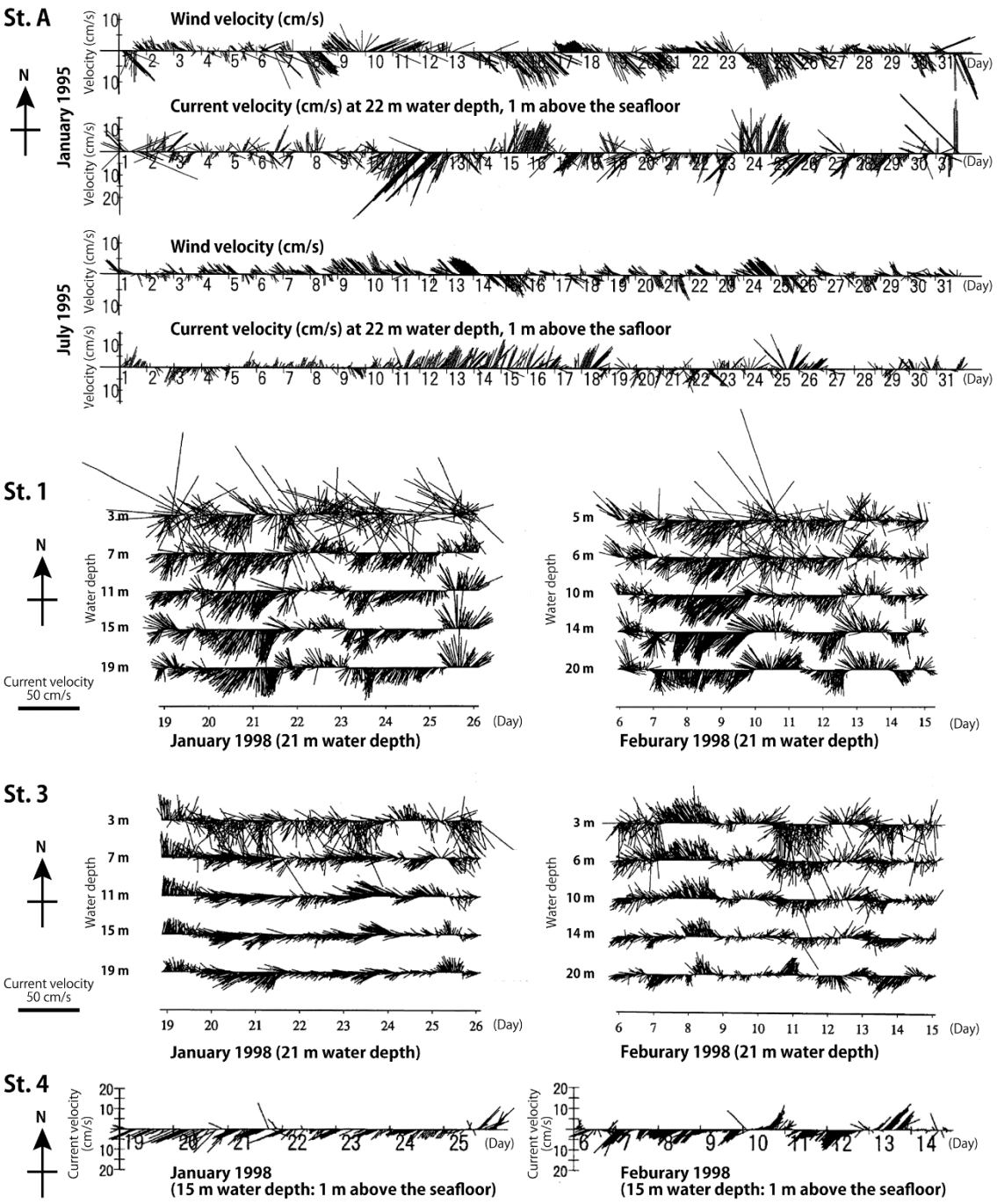

709

710 Fig. 3 Directions and velocities of wind-driven currents in the Ishikari Bay measured using
711 acoustic Doppler current profiler (after Yamashita et al., 1998; 1999). The wind condition
712 at St.A is also shown. The current velocities at St. A were measured at 40 seconds interval,
713 at St. 1 and St. 3 were at 10 minutes interval, and at the St. 4 were at 0.5 second interval
714 for 20 minutes of every hour. These figures are reprinted with permission from the Japan
715 Society of Civil Engineers. See Figure 1 for observation locations.

716

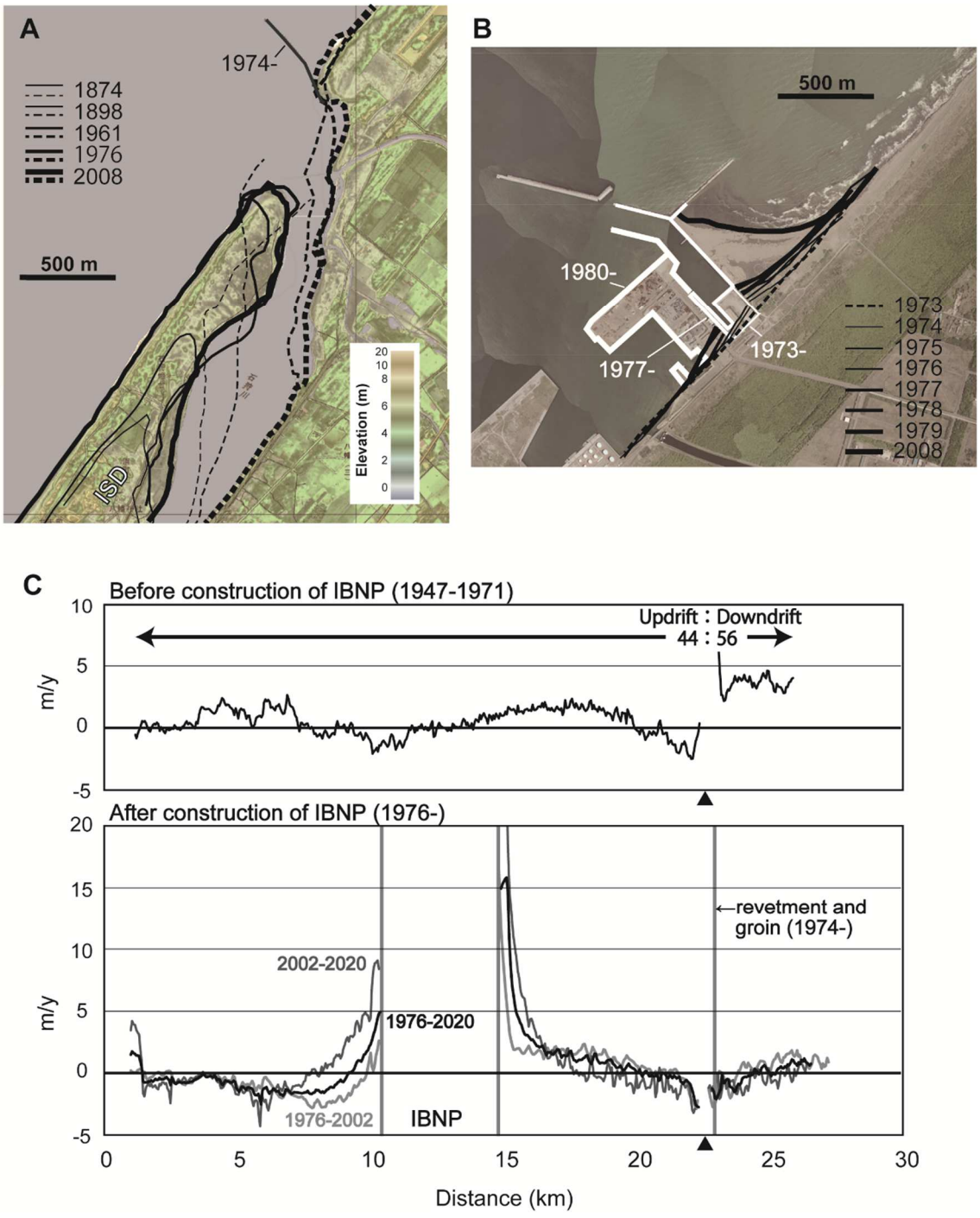

Fig. 4 (A) Growth history of the river mouth spit based on the aerial photos (modified from Yamazaki and Yamashita, 2004). (B) Prograding coastline at the artificial groin (IBNP) (modified from Arai, 1981). (C) Chronological transition of the entire Ishikari sandy coastline before and after the construction of IBNP, showing the distributed ratio of accreted sediments during 1947–1971. The black triangle shows the location of the Ishikari river mouth. The aerial photo and the digital elevation model are provided by the Geospatial Information Authority of Japan.

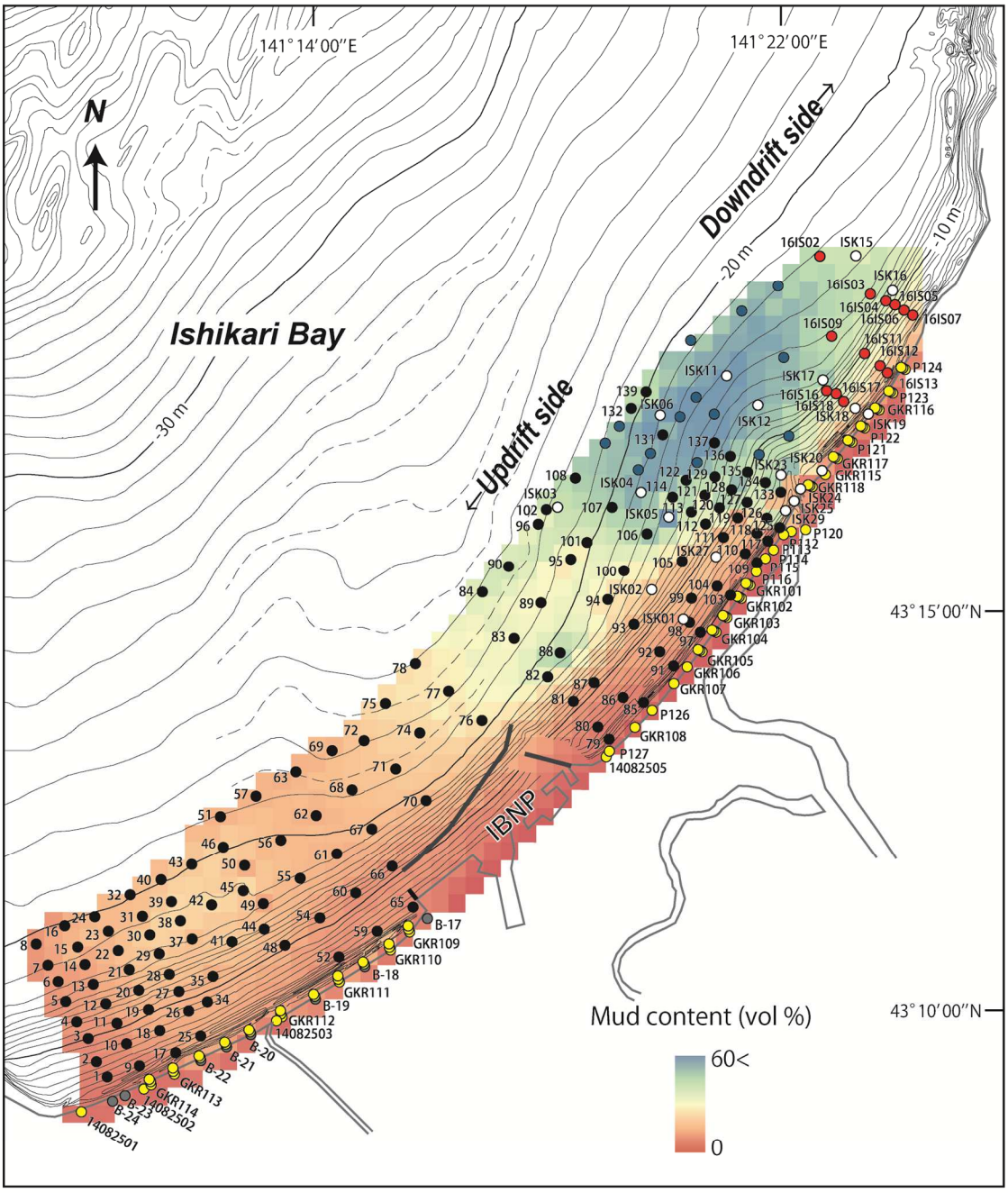

Fig. 5 Location and survey year of the collected samples in Ishikari coast. Suffix beside the circles shows sample code in the source. The colour gradients show the spatial variation of the mud content in the seafloor sandy sediments, as estimated by Kriging interpolation (400-m grid).

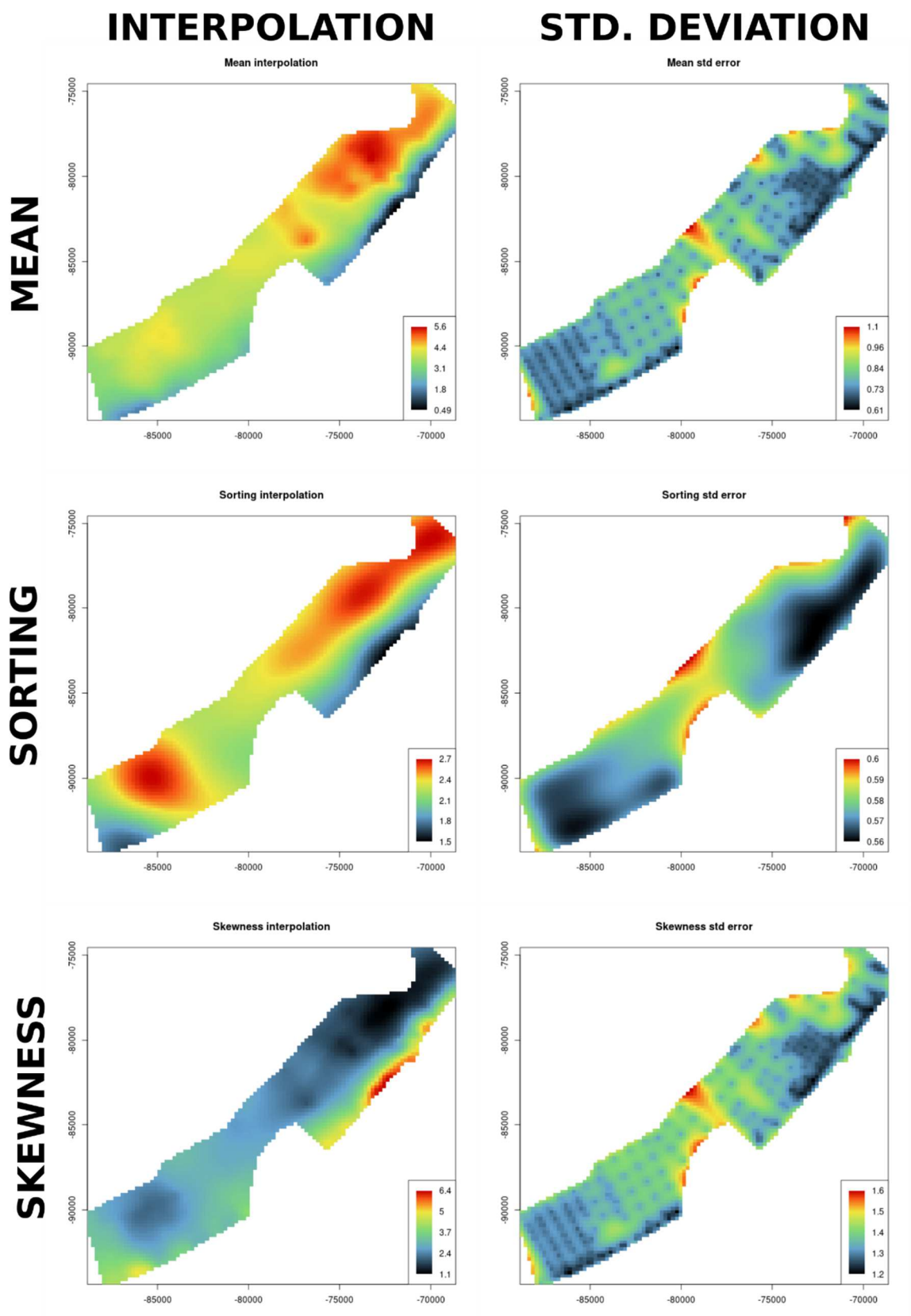

732

Fig. 6 Interpolations of the three statistical parameters (left column) and the variance of the interpolation error (right column), of respectively mean, sorting and skewness.

733

734

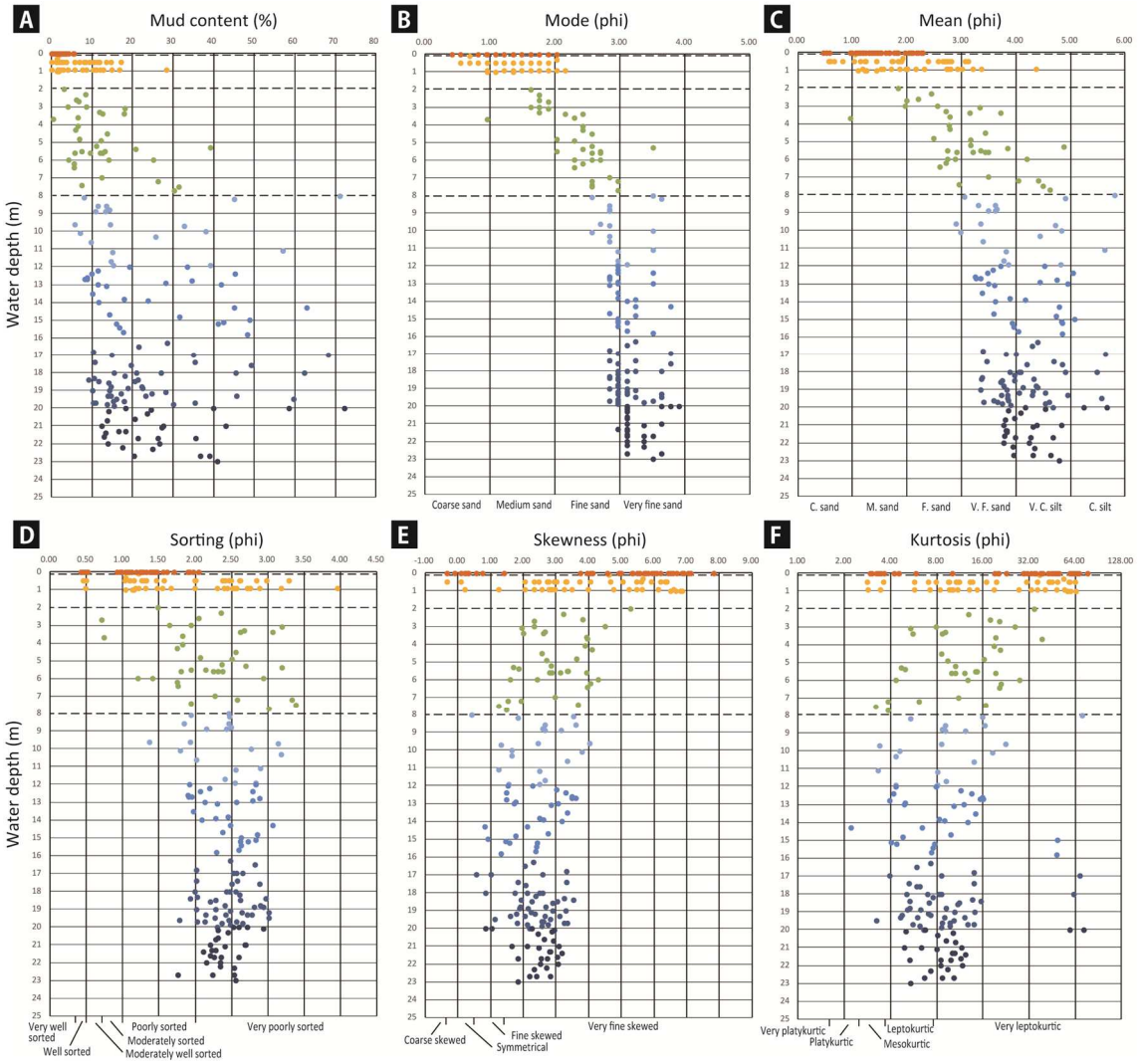

Fig. 7 Grain-size composition of seafloor sediments analysed via logarithmic method of moments: values of mud content (A), and statistical grain-size parameters (mode (B); mean (C); sorting (D); skewness (E); and kurtosis (F)) versus water depth. The key to colour is same as the Fig. 8.

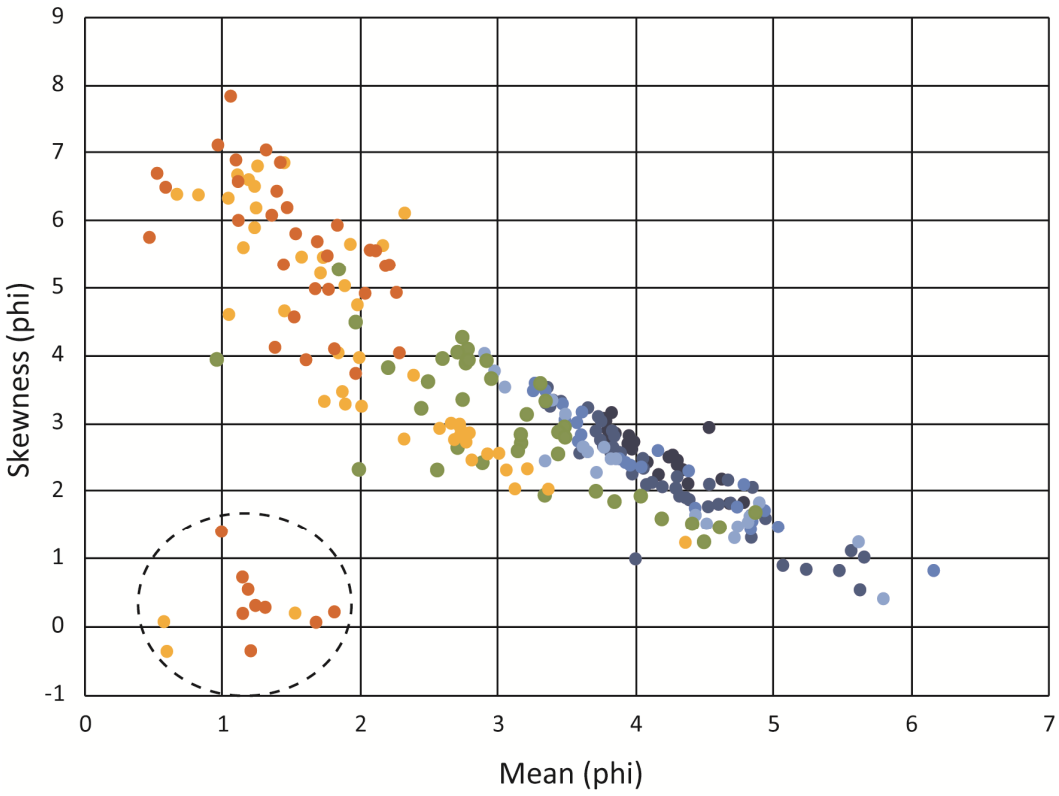

743

744 Fig. 8 Relationships between the value of mean and skewness of analysed seafloor sediments.

745 The key to colour is same as the Figure 8. The samples circled by dotted line were not

746 used for the interpolation and the GSTA analysis.

747

748

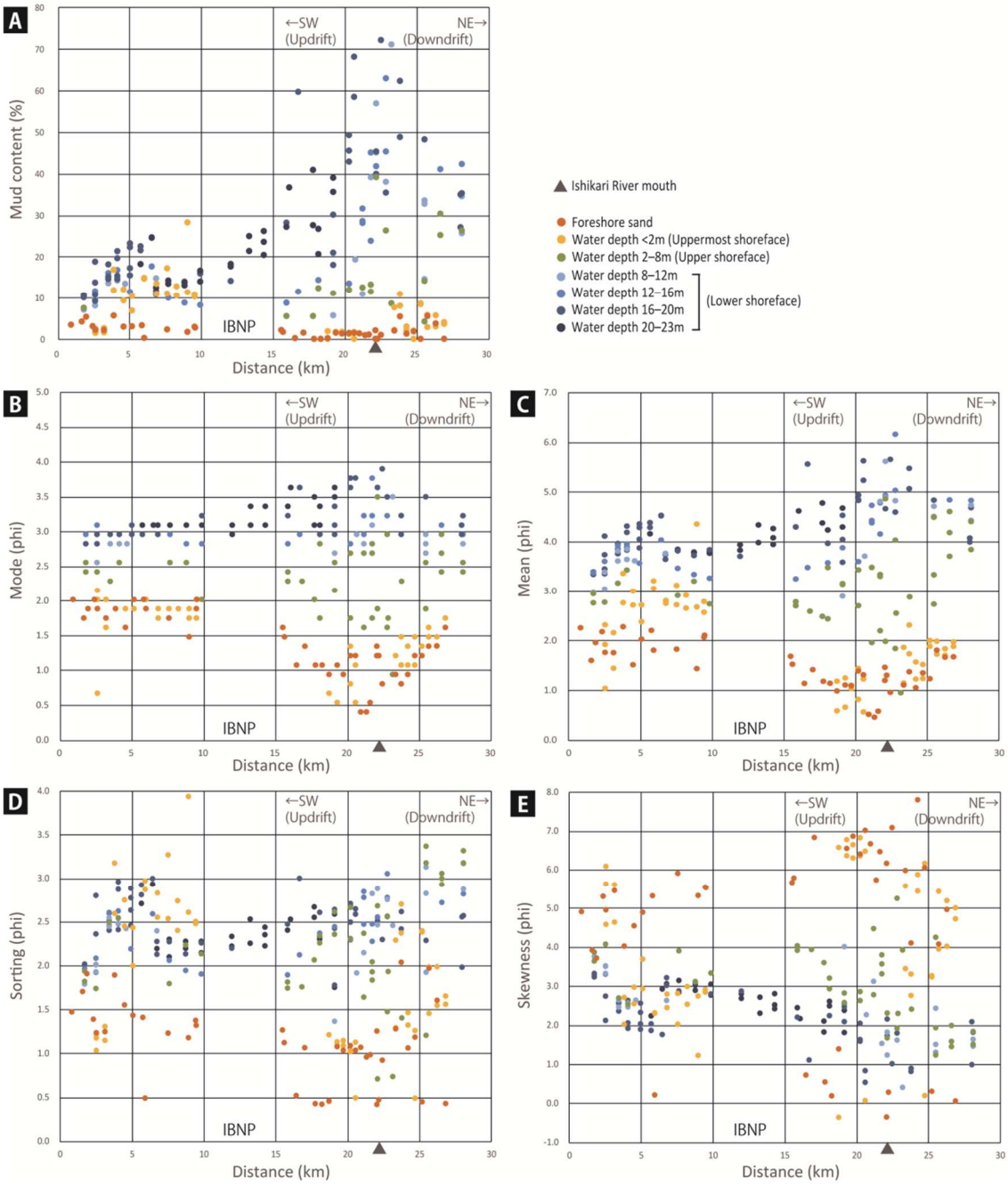

749

750 Fig. 9 Alongshore spatial variation of mud content (A) and statistical grain-size parameters
751 (mode (B); mean (C); sorting (D); and skewness (E)) of seafloor sediments. The distance
752 is from the western end of the sandy coast (mouth of the Zenibako-gawa River, see Fig. 1
753 for location).

754

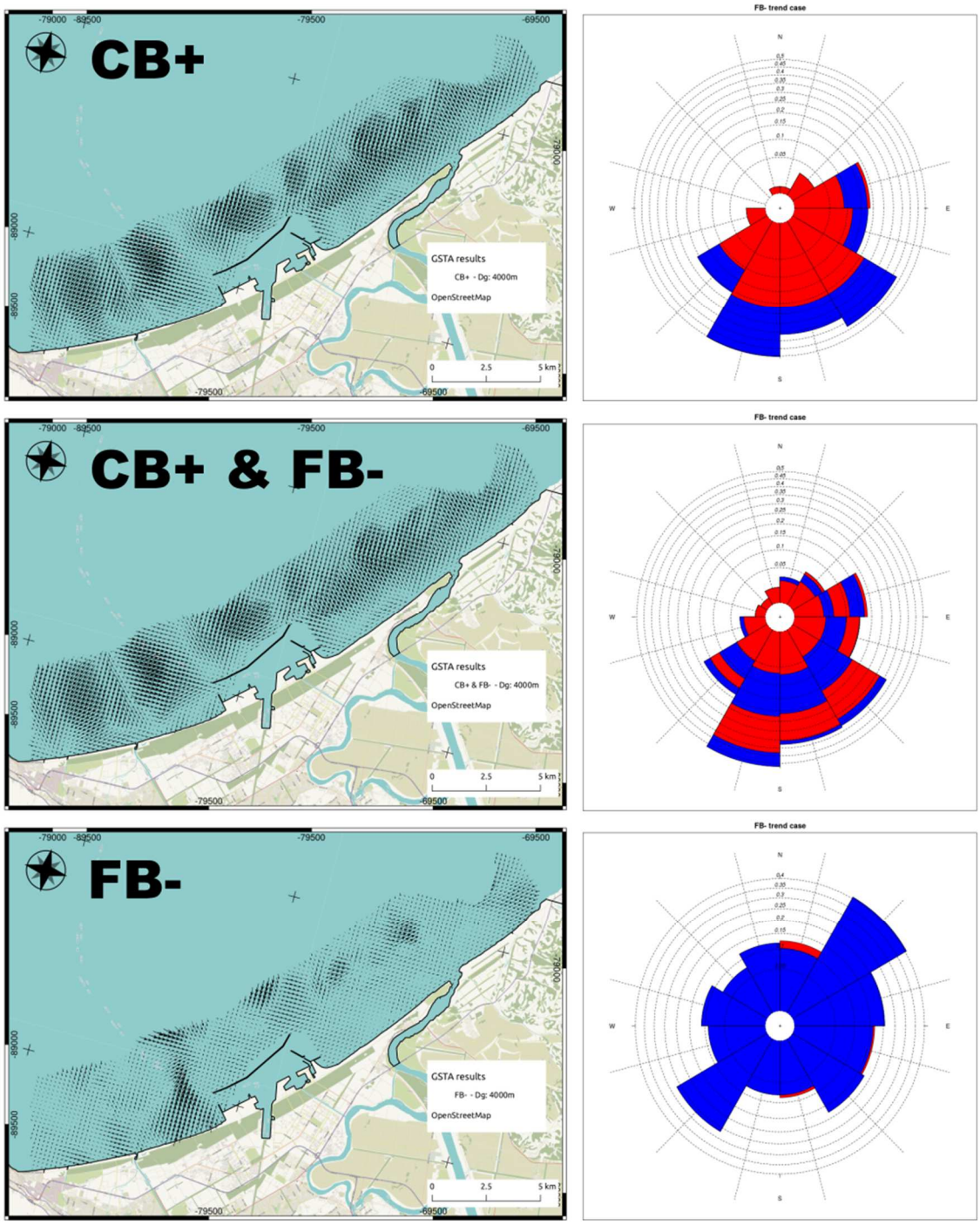

Fig. 10 Results of GSTA using GiSedTrend. Vector fields (left column) and windrose diagrams (right column), for respectively CB+, CB+ & FB- and FB- trend cases.

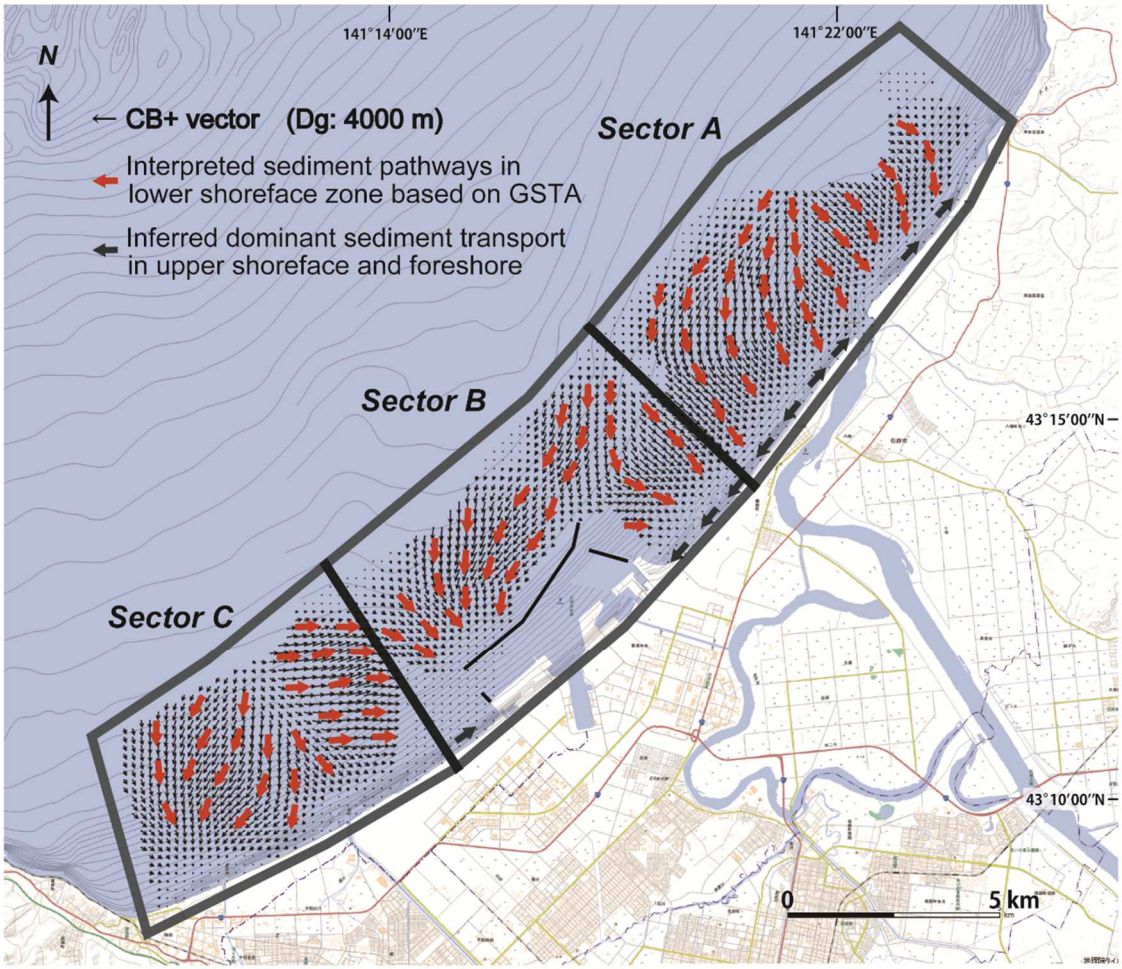

759

760 Fig. 11 Three different areas recognized on the CB+ trend case vector field, respectively A, B

761 and C. Red arrows correspond to main transport directions.

762

763

764

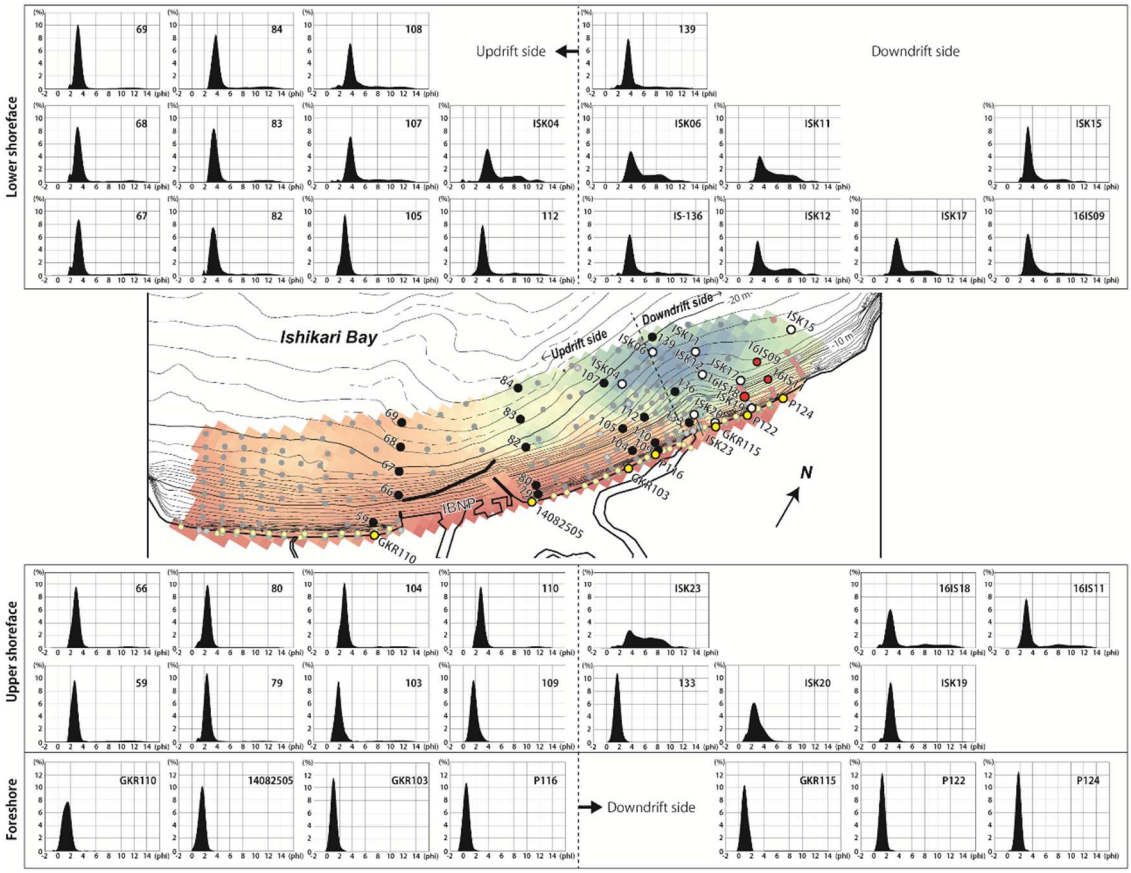

765

766 Fig. 12 Representative histograms of analysed sediment samples on a logarithmic scale (phi).
767 The enlarged circles on the inset map show the sampling sites. The dashed line at the
768 centre of the river mouth extending seaward represents approximate boundary line
769 between the updrift and downdrift sides. The colour gradient represents the spatial
770 distribution of the mud content.

771

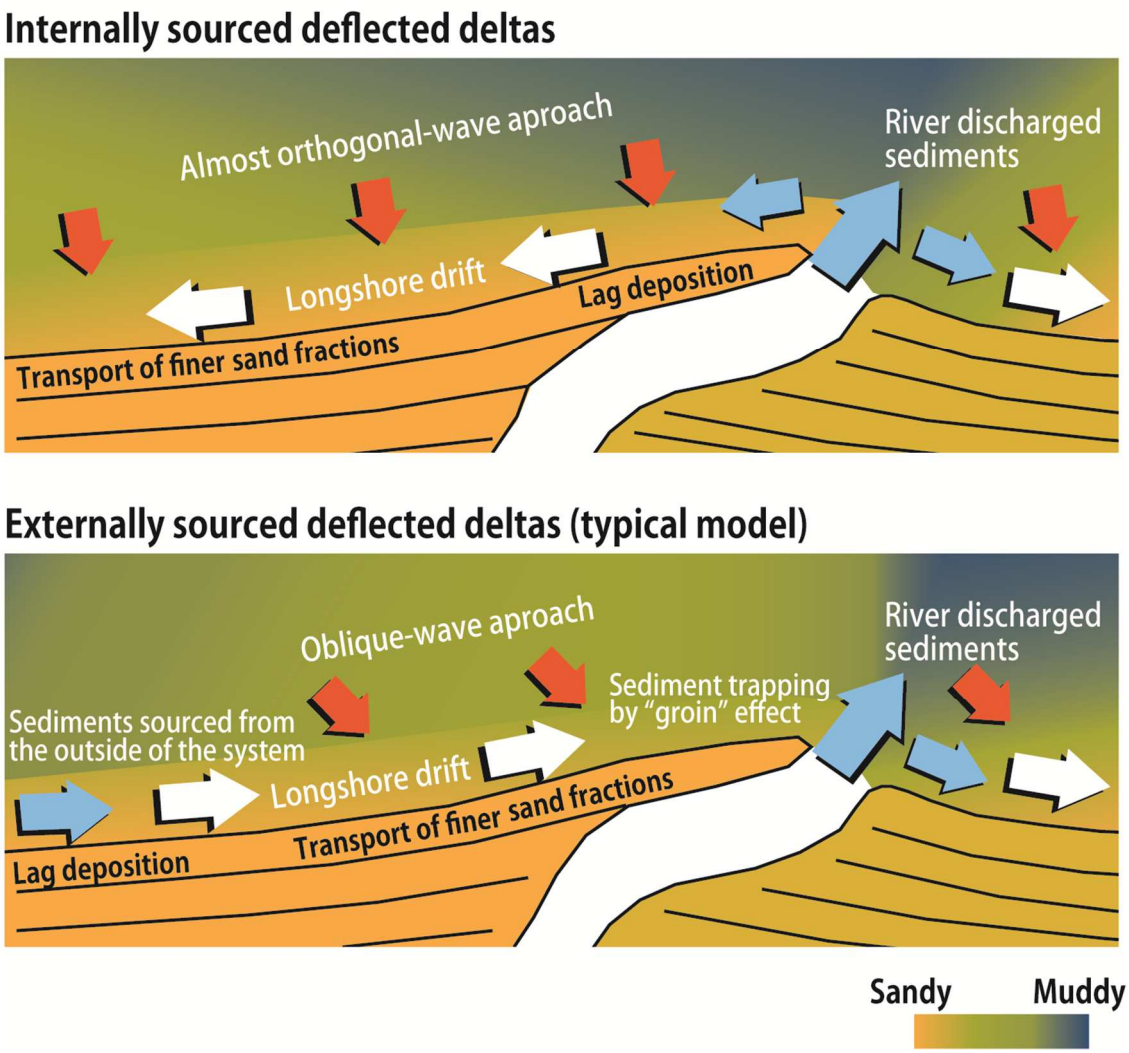

772

773 Fig. 13 Comparison of sediment dynamics of internally sourced and externally sourced
774 deflected delta systems. Externally sourced deflected deltas (lower) grow under
775 net-downdriftward sediment transport, whereas the growth of internally sourced
776 deflected deltas (upper) depends on dominant updriftward sediment transport on
777 the updrift-side.

778

779